Plasma MIR-212-3p as a biomarker for acute right heart failure with pulmonary artery hypertension

Yue Yang[1], Renhua Li[1], Yanan Cao[1], Sisi Dai[1], Sumei Luo, Qulian Guo[1], E. Wang[1,2,3]^

[1]Department of Anesthesiology, Xiangya Hospital Central South University, Changsha, China; [2]National Clinical Research Center for Geriatric Disorders, Xiangya Hospital Central South University, Changsha, China; [3]Key Laboratory of Biological Nanotechnology of National Health Commission, Changsha, China

Contributions: (I) Conception and design: E Wang, Y Yang; (II) Administrative support: E Wang, Q Guo; (III) Provision of study materials or patients: E Wang, S Luo, S Dai; (IV) Collection and assembly of data: R Li, S Dai; (V) Data analysis and interpretation: Y Cao; (VI) Manuscript writing: All authors; (VII) Final approval of manuscript: All authors.

Correspondence to: E. Wang. Department of Anesthesiology, Xiangya Hospital Central South University, Changsha, China. Email: ewang324@csu.edu.cn.

Background: Acute right heart failure occurs in patients with pulmonary artery hypertension (PAH) with exposure to acute inflammation, the mortality rate is very high when right heart failure occurs. Biomarkers that can be used to detect acute right heart failure in patients with pulmonary hypertension need to be studied.

Methods: A PAH rat model was established using monocrotaline, and lipopolysaccharide was used to induce acute right heart failure. The Agilent rat miRNA microarray, Gene Ontology (GO) analysis and Kyoto Encyclopedia of Genes and Genomes (KEGG) analysis were used to assess the microRNA expression of PAH rats. The expression of up- and downregulated miRNAs in plasma from PAH patients with acute right heart failure was validated with quantitative reverse transcription polymerase chain reaction (qRT-PCR). Then, the Wilcoxon matched paired test and receiver operating characteristic (ROC) curve analysis were performed.

Results: Thirty-three miRNAs were upregulated, and 7 miRNAs were downregulated in plasma of PAH rats with acute right heart failure. In the plasma of PAH patients, the miR-212-3p level was inversely correlated with the level of NT-pro BNP, and the area under the ROC curve was 0.751.

Conclusions: These results suggest that the reduction of the expression of MIR-212-3p may be a biomarker for PAH patients with right heart dysfunction.

Keywords: microRNA; right heart failure; pulmonary hypertension; inflammation

Introduction

In clinical practice, patients with stable pulmonary hypertension are prone to acute right heart failure due to acute inflammation. The in-hospital mortality of patients with pulmonary hypertension who developed acute right heart failure was reported to be 41% (1). In our previous study, we used monocrotaline to establish a pulmonary artery hypertension (PAH) rat model and simulated acute inflammation with intraperitoneal injections of lipopolysaccharide (LPS). We found that a nonlethal dose of LPS caused acute right heart failure and death in rats with PAH (2). To date, there is no effective medical treatment or monitoring indicator for acute right heart failure occurring in patients with PAH.

---

^ ORCID: 0000-0001-9463-9769.

MicroRNAs inhibit the translation of messenger RNA (mRNA) and induce the degradation of specific mRNA to regulate gene expression at the posttranscriptional level (3). In the past few years, circulating microRNAs have been investigated as biomarkers of disease in the diagnosis and prognosis of various conditions. Some cardiac-specific miRNAs, such as miR-1, miR-133a and miR-208a, have also been shown to play important roles in maintaining heart development and function (4-6). The increased level of circulating miR-195-3p could be a potential biomarker for heart failure (HF) (7). In addition, miR-302b-3p levels were significantly higher in patients with left ventricular ejection fraction ≤45% and in New York Heart Association class IV than in other patients and could be potentially applied for acute heart failure (AHF) diagnosis (8). A recent study also showed that the serum circulating miR-150 level was independently associated with acute myocardial infarction (AMI) and is a novel biomarker for predicting post-AMI HF (9). To date, biomarkers for detecting acute right heart failure in patients with pulmonary hypertension are still lacking.

In this study, we detected the miRNA expression profile in plasma from rat models of PAH and acute right heart failure. The expression of upregulated and downregulated microRNAs was verified in plasma of PAH patients with acute right heart dysfunction. We hypothesized that certain microRNAs could predict or diagnose acute right heart failure in PAH patients. We present the following article in accordance with the ARRIVE reporting checklist (available at http://dx.doi.org/10.21037/atm-20-1653a).

Methods

Samples obtained from rats and patients

The PAH rat model was induced as previously described(10). Briefly, male Sprague-Dawley rats that weighed 250–300 g (Laboratory Animal Center of Central South University, Changsha, China) were given a single intraperitoneal injection of 1% monocrotaline (60 mg/kg, Sigma-Aldrich, St. Louis, MO). After 4 weeks, pulmonary arterial pressure was measured by echocardiography. Every 2 days, we used ultrasound to measure PAP of the rats and the rats were assigned to the next experiment when PAP reached 60 mmHg. The rats were randomly divided into groups with or without LPS treatment. Rats of the LPS group were given intraperitoneal injections of normal saline or LPS (1 mg/kg, serotype O55:B5, Sigma-Aldrich,

St. Louis, MO). Six hours later, echocardiography was performed again to assess right heart dysfunction (10). All rats were given ketamine anesthesia, and blood samples were extracted. The protocol was approved by the Ethics Committee for Animal Research of Xiangya Hospital of Central South University (permit number: 201711997) and all experiments were cared for in accordance with the recommendations of national and international animal care and ethical guidelines. The plasma BNP levels of rats were detected with a double-antibody sandwich enzyme-linked immunosorbent assay (ELISA) (E-EL-R0126c, Elabscience Biotechnology Co., Ltd., Wuhan, China) in accordance with the manufacturer's instructions.

Blood samples were obtained from PAH patients of Han Chinese nationality with acute right heart failure for the validation study. Individuals who met the following criteria were included: patients with pulmonary hypertension and right heart dysfunction diagnosed by echocardiography or right cardiac catheterization, and patients suffering acute infectious disease or inflammation after cardiac or obstetric surgery. The blood samples of PAH patients undergoing valve surgery were collected. Demographic and clinical data, including age, sex, and serum biochemistry parameters, were collected. The study was conducted in accordance with the Declaration of Helsinki (as revised in 2013). The study was approved by the Institutional Review Board and Ethics Committee of Xiangya Hospital Central South University (201303311), and informed consent was obtained from patients.

All blood samples were centrifuged at 3,000 ×g for 10 min at room temperature, and the obtained serum samples were stored at –80 ℃ for RNA extraction.

Morphologic study

After the rats were euthanized, their hearts were harvested and fixed with 4% paraformaldehyde. The midventricular slice was used to estimate the ratio of right ventricular over left ventricular wall thickness using an image analysis program. Morphological changes of the myocardium of right ventricle from control rats and PAH rats were assessed by haematoxylin and eosin staining.

RNA extraction

Total RNA was extracted from plasma samples of rats and patients, and a mirVanaTM PARISTM Kit (AM1556,

Ambion, TX) was used according to the manufacturer's protocol. First, 625 µL of each sample was mixed with an equal volume of 2X Denaturing Solution at room temperature. Then, 1/3 volume 100% ethanol was added to the aqueous phase, mixed thoroughly, and centrifuged for 30 s to collect the filtrate. After washing the filter twice with Wash Solution, 100 µL of preheated (95 ℃) Elution Solution was applied to the center of the filter, and the eluate (containing the RNA) was collected and stored at −80 ℃. The quality of total RNA was assessed with Agilent 2100 bioanalyzer (Agilent Technologies, USA) and the results are shown in Figure S1.

Microarray analysis

For each sample, 100 ng of RNA was dephosphorylated for the 16 ℃ labeling reaction, after which, the samples were dried completely. Then, the 10× Blocking Agent was prepared with an Agilent miRNA Complete Labeling and Hyb Kit (p/n 5190-0456). The microarray was incubated at 55 ℃ for 20 hours to hybridize and wash it. Next, the microarray was scanned, and images were then imported into Feature Extraction software for grid alignment and data extraction. The data were normalized using the quantile method using Genespring software. After normalization, significant differentially expressed (DE) miRNAs were identified through volcano plot filtering, and a heatmap was generated to show distinguishable miRNA expression profiles among samples. miRNAs with a fold change >1.5 and a P value <0.05 were considered to be differentially expressed.

Bioinformatic analysis

The predictions of target genes of miRNAs were conducted using the prediction algorithm GeneSpring13.1. TargetScan and microRNAorg were used to predict target genes of differentially expressed miRNAs. Taking an intersection of the two databases, we utilized GO (Gene Ontology) analysis and KEGG (Kyoto Encyclopedia of Genes and Genomes) pathway analysis to perform annotations of predicted target genes. The GO consists of Biological Process, Cellular Component and Molecular Function. False discovery rate (FDR = adjusted P values) values <0.05 for GO and KEGG pathway analysis were considered statistically significant.

Reverse transcription-quantitative polymerase chain reaction (RT-qPCR)

For validation of differentially expressed miRNAs, total RNA was extracted from plasma samples of patients following the instructions. For reverse transcription, 1 µg of total RNA was used for each sample according to the protocol to generate first-strand cDNAs. qRT-PCR was performed on an ABI 7900 system (Applied Biosystems, Carlsbad, CA) by using a SYBR Premix Ex TaqTM II kit (DRR820A, TaKaRa, Japan). The PCR program was 95 ℃ for 30 s, 40 cycles of 95 ℃ for 5 s and 60 ℃ for 34 s, 95 ℃ for 15 s, 60 ℃ for 1 min, and 95 ℃ for 15 s. The expression level of miRNAs was normalized to U6 snRNA in each sample and calculated using $2^{-\Delta\Delta Ct}$. The primers used for qPCR detection and their sequences are provided below:

5'-3'
MIR-212-3p→TAACAGTCTCCAGTCACGGC
MIR-29a-3p→TAGCACCATCTGAAATCGGTTA
MIR-494-3p→TAACAGTCTCCAGTCACGGC
MIR-127-5p→TAGCACCATCTGAAATCGGTTA
MIR-106b-5p→TGCGGCAACACCAGTCGATGG
let-7f-5p→CTATACGACCTGCTGCCTTTC
let-7d-3p→CTATACGACCTGCTGCCTTT

Statistical analysis

SPSS 23.0 software (IBM, NY) and GraphPad Prism 6.0 (GraphPad Software, CA) were used for statistical analyses. The results are presented as the mean ± standard deviation (SD), and Student's t-test was selected to compare differences between the groups. The Wilcoxon matched paired test was used to compare the miRNA levels of 15 patients before and after surgery. Because the expression levels of miRNAs were significantly different, receiver operating characteristic (ROC) curves were established, and the area under the curve (AUC) was calculated to assess the diagnostic potential of these miRNAs. A value of P<0.05 was considered to denote statistical significance.

Results

Identification of differentially expressed miRNAs in plasma of PAH rats with or without LPS treatment

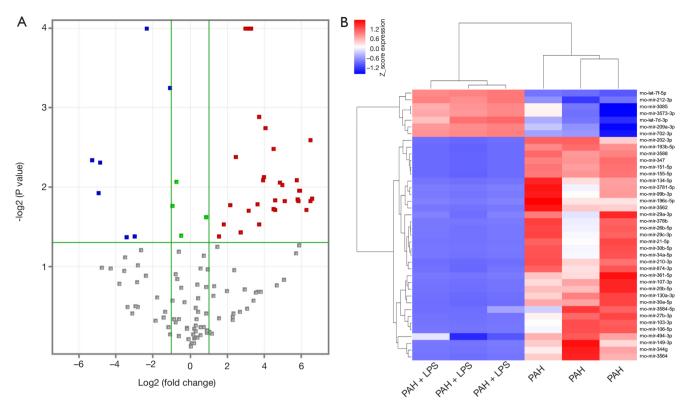Myocytes of RV fractured with cytoplasm swelling and

Figure 1 The expression of miRNAs in plasma between PAH rats with LPS treatment and PAH rats without LPS treatment. (A) Differences in miRNA expression in the plasma between the two groups of rats are shown by a volcano plot. Red dots represent the downregulated miRNAs, and blue dots represent the downregulated miRNAs; (B) Heat map of differentially regulated miRNAs from plasma samples of PAH rats (n=3) and PAH rats treated with LPS (n=3) as identified by microarray. MiRNAs and subjects are hierarchically clustered by Manhattan distance on the y and x axes, respectively. The relative miRNA expression is depicted according to the color scale shown on the right. Blue and red indicate fold changes as low and high, respectively. PAH, PAH rats; PAH+LPS, PAH rats treated with LPS.

hypertrophy in PAH rats when compared with normal rats (Figure S2). Ventricular function in the rat model and LPS-induced right heart failure were detected by echocardiography, and the data are shown in Table S1. After LPS treatment, the tricuspid annular plane systolic excursion (TAPSE) was significantly decreased, and the right ventricle end-diastolic diameter (RVEDD) and sPAP were increased in PAH rats. The strains of the basal and middle segments of the RV free wall and the basal segments of the septal wall were reduced after LPS injection. The level of BNP was significantly higher in the LPS-treated PAH group than in the PAH group. After microarray detection, the raw data were normalized and summarized. The miRNAs that could discriminate between the PAH group and the PAH+LPS group were identified. As displayed by a volcano plot (*Figure 1A*), on

the basis of the criteria (P≤0.05 and |FC| ≥2), microarray analysis demonstrated that 33 miRNAs were upregulated and 7 miRNAs were downregulated in the plasma of PAH rats with acute right heart failure compared with the expression in PAH rats without LPS treatment. A heatmap illustrating the distribution of differential miRNAs between the two groups is displayed in *Figure 1B*. The up- and downregulated miRNAs are listed in *Table 1*.

Functional and pathway enrichment analysis of predicted target genes by GO and KEGG

Target genes were predicted with TargetScan and microRNAorg data. The software GeneSpring13.1 was used for selecting target gene prediction, and a Venn diagram (*Figure 2A*) shows the number of differentially

Table 1 MicroRNAs were significantly up- and downregulated in the plasma of PAH rats with or without LPS treatment

miRNA	Regulation direction	Fold change (Log FC)	P value
rno-mir-212-3p	Down	−1.0900412	0.0006
rno-let-7f-5p	Down	−2.3343024	0.0001
rno-mir-3573-3p	Down	−3.0048778	0.0412
rno-mir-3085	Down	−3.417509	0.0422
rno-let-7d-3p	Down	−4.8408146	0.0049
rno-mir-409a-3p	Down	−4.9554386	0.0120
rno-mir-702-3p	Down	−5.289188	0.0046
rno-mir-34a-5p	Up	6.5509987	0.0138
rno-mir-210-3p	Up	6.473572	0.0025
rno-mir-30b-5p	Up	6.462021	0.0151
rno-mir-378b	Up	6.2248945	0.0192
rno-mir-103-3p	Up	5.9058046	0.0111
rno-mir-21-5p	Up	5.870143	0.0110
rno-mir-106b-5p	Up	5.791479	0.0150
rno-mir-29c-3p	Up	5.7560463	0.0144
rno-mir-27b-3p	Up	5.7053404	0.0083
rno-mir-344g	Up	5.084838	0.0151
rno-mir-134-5p	Up	4.934724	0.0094
rno-mir-107-3p	Up	4.809766	0.0089
rno-mir-149-3p	Up	4.5719647	0.0192
rno-mir-3562	Up	4.5494337	0.0147
rno-mir-130a-3p	Up	4.4843936	0.0033
rno-mir-361-5p	Up	4.4605274	0.0190
rno-mir-202-3p	Up	4.058842	0.0018
rno-mir-20b-5p	Up	3.9460397	0.0074
rno-mir-3564	Up	3.9295	0.0081
rno-mir-30e-5p	Up	3.708817	0.0013
rno-mir-378a-5p	Up	3.6807606	0.0295
rno-mir-26b-5p	Up	3.6092956	0.0164
rno-mir-347	Up	3.2823017	0.0000
rno-mir-193b-5p	Up	3.222711	0.0000
rno-mir-3588	Up	3.2092464	0.0000
rno-mir-99b-3p	Up	3.137311	0.0198
rno-mir-151-5p	Up	3.1003902	0.0000
rno-mir-155-5p	Up	2.9728086	0.0000
rno-mir-196c-5p	Up	2.7101727	0.0372
rno-mir-874-3p	Up	2.4486141	0.0042
rno-mir-494-3p	Up	2.1411104	0.0169
rno-mir-29a-3p	Up	1.7845945	0.0292
rno-mir-3584-5p	Up	1.5302668	0.0422

expressed predicted target genes with 2 databases. A GO enrichment analysis (*Figure 2B*) of the predicted target genes showed that they were mainly related to molecular function, and only a few genes were associated with biological processes and cellular components. The genes were obviously enriched in protein binding, protein kinase binding, aging, response to drug, cytoplasm and cytosol. KEGG pathway enrichment analysis (*Figure 2C*) indicated that these predicted target genes were significantly enriched in different pathways, such as the HIF-1 signaling pathway (KEGG: 04066), cGMP-PKG signaling pathway (KEGG: 04022), FoxO signaling pathway (KEGG: 04068), adipocytokine signaling pathway (KEGG: 04920) and so on.

Circulating miRNAs as new biomarkers for detecting changes in right heart function in patients

According to the GO and KEGG analysis, 7 miRNAs (Mir-494-3p, Mir-127-5p, Mir-29a-3p, let-7d-3p, Mir-212-3p, let-7f-5p, and Mir-106b-5p) related to cardiac function were chosen for validation. We also screened whether these miRNAs were blood-enriched and cardiac-enriched miRNAs among these 7 differentially expressed miRNAs. The screened miRNAs were tested by qPCR; only MiR-29a-3p and MiR-212-3p were detected in the plasma of patients, and others were not detected. We performed follow-up studies with plasma MiR-29a-3p and MiR-212-3p levels in 15 included PAH patients, and we used the level of NT-pro BNP in plasma as an indicator of cardiac function. Among the 15 patients (*Table 2*), 12 had increased levels of NT-pro BNP (Table S2). As shown in *Figure 3A*, the plasma MiR-212-3p levels in 15 patients were markedly decreased after surgery (Wilcoxon matched paired test, P=0.015). Importantly, for the 12 patients with increased NT-pro BNP, the level of this marker was markedly decreased after surgery (Wilcoxon matched paired test, P=0.048), but for the 3 patients who did not have increased NT-pro BNP, the plasma MiR-212-3p levels did not change significantly before or after surgery (Wilcoxon matched paired test, P=0.23).

We also assessed plasma MiR-29a-3p levels, and the P value was 0.61 (*Figure 3B*), indicating that MiR-29a-3p could not serve as a biomarker.

Discriminatory potential of circulating MiR-212-3p for the decrease in cardiac function by ROC analysis

Receiver operating characteristic analysis was performed to determine the sensitivity and specificity of MiR-212-3p for heart failure prediction. As shown in *Figure 4*, the ROC curves of miR-212-3p revealed its probability as a valuable biomarker with an area under the curve (AUC) of 0.751 (*Table 3*). Moreover, to obtain the best diagnostic sensitivity and specificity, a cutoff point was used for further analysis, showing a sensitivity of 86.7% and accuracy of 66.7%, indicating the predictive value for reduced heart function.

Discussion

PAH is a complex process that involves atrial function, inflammation, and vasoconstriction. Once pulmonary vascular resistance increases and the impairment of pulmonary arterial compliance appears, the right atrium attempts to compensate for the increased afterload. When sudden inflammation is present, right ventricle (RV) dilatation and systolic dysfunction occur, leading to right heart failure and death (11). RV dysfunction is an important prognostic factor in PAH and is the main cause of death in PAH patients (12). In patients older than 65 years, acute heart failure (AHF) is a leading cause of hospitalization and mortality (13). Therefore, RV dysfunction has emerged as an important research priority in the field of cardiopulmonary research. Small studies have shown that the prognostic value of pulmonary hypertension (PH), as estimated by echocardiography in patients with AHF, suggests incremental prognostic information and poor prognosis (14).

In our collection of preoperative and postoperative data on patients with pulmonary hypertension, we found that the patients without infection before operation had increased leukocyte and higher NT-proBNP levels after surgery. We used monocrotaline to establish a rat model of pulmonary hypertension, and LPS was used to induce acute right heart failure. In our present study, we investigated miRNA expression profiles and showed that 33 miRNAs were upregulated and 7 miRNAs were downregulated in the plasma of PAH rats with acute right heart failure. To our knowledge, no study has directly compared these miRNAs in acute right heart failure with PAH. Using a rat model and patient plasma samples, we assessed the release of miRNAs after acute inflammation based on PAH and miRNAs in the most relevant clinical signs of acute right heart failure. Our results revealed that PAH patients showed lower levels of miR-212-3p in plasma after surgery than before surgery. Moreover, the level of plasma miR-212-3p correlated with the clinical features of poor heart function.
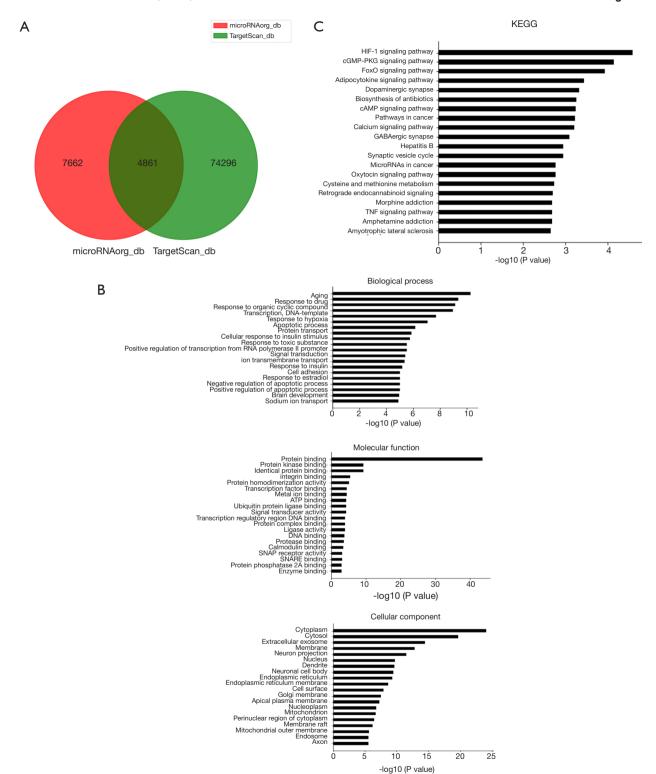
Figure 2 Functional and pathway enrichment analysis of predicted target genes. (A) The Venn diagram demonstrates the number of the predicted target genes of detected miRNAs with two databases; (B) GO analysis of target genes of differentially expressed miRNAs; (C) KEGG pathway analysis of target genes of differentially expressed miRNAs. The abscissa is the –Lg P value (–LgP), and the larger the –LgP, the smaller the P value is.

Table 2 Characteristics and laboratory indicators of PAH patients of the Han nationality

Variable	Before surgery	After surgery	P value
Age, y	54.6±12.8	54.6±12.8	
Male/female (n)	7/8	7/8	
sPAP, mmHg	59.2±15.6	NA	
WBC (×10^9/L)	5.9±2.4	14.3±4.4	<0.001
NEUT (×10^9/L)	3.4±1.8	12.5±3.9	<0.001
LYM (×10^9/L)	1.7±0.7	0.7±0.3	<0.001
MONO (×10^9/L)	0.5±0.2	1.1±0.6	0.002
NT-proBNP (pg/mL)	2,402.7±2,508.9	3,234.9±2,266.7	0.03

WBC, white blood cell count; NEUT, neutrophil count; LYM, lymphocyte; MONO, monocyte counts; NT-proBNP, N-terminal of the prohormone brain natriuretic peptide; NA, not available.
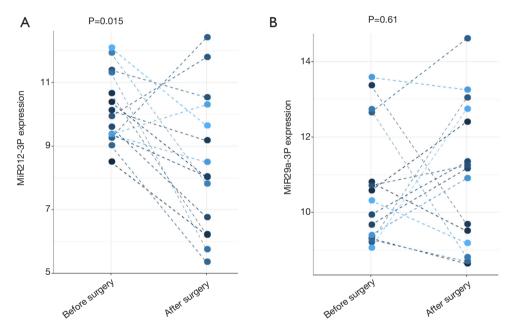

Figure 3 Plasma levels of MiR-212-3p and MiR-29a-3p in PAH patients before and after surgery. (A) Plasma levels of MiR-212-3p in PAH patients before and after surgery; (B) Plasma levels of MiR-29a-3p in PAH patients before and after surgery. Left, n=15; middle, n=12; right, n=3.

The differentially expressed miRNAs identified from the microarray analysis were related to many pathological processes. We selected 7 miRNAs based on bioinformatics predictions related to heart function. A previous study indicated that the level of miR-494-3p was significantly upregulated in the myocardium of diabetic rats compared with that of the control rats. Furthermore, the level of miR-494-3p in H9C2 cells cultured in high-glucose and high-fat medium was also significantly increased, whereas the downregulation of miR-494-3p led to an increase in insulin-stimulated glucose uptake and the ratio of p-Akt/Akt. We can see that miR-494-3p reduces insulin sensitivity in diabetic cardiomyocytes (15). Another study showed that miR-494-3p was downregulated in hearts from obese mice, while its overexpression prevented lipotoxic damage. MiR-494-3p was also dysregulated in myocardial specimens from obese patients compared with those from nonobese controls and was correlated with echocardiographic indices of
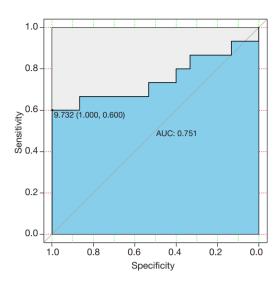
Figure 4 Receiver operating characteristic (ROC) curves were drawn with the fold change data of plasma MiR-212-3p from 15 PAH patients. The AUC curve of MiR-212-3p is was 0.751. The dashed line indicates the "random guess" diagonal line. AUC indicates area under the curve.

Table 3 Receiver operator characteristic curve (ROC) analysis of MiR-212-3p

ROC characteristic	MiR-212-3p
AUC	0.751
Standard error	0.097
95% confidence interval	0.562 to 0.941
Significance level P (area =0.5)	0.019

LV dysfunction (16). MiR-106b-5p was identified by RNA sequencing as one of the key miRNAs related to sepsis (17). In addition, the most significant differences in miR-106b-5p are between patients with atherosclerosis and individuals without atherosclerotic disease, and this miRNA targets multiple signaling pathways in vascular endothelial cells, such as tumor necrosis factor (TNF), Toll-like receptor (TLR), hypoxia-inducible factor 1α (HIF-1α) and other signaling pathways (18). Circ_0136474 suppressed the expression of miR-127-5p, resulting in the suppression of cell proliferation by facilitating MMP-13 expression, and overexpression of miR-127-5p negatively regulated MMP-13 expression and enhanced cell proliferation (19). Studies have shown that the expression of rno-let-7d-3p is decreased in patients with amyotrophic

lateral sclerosis compared with healthy controls (20), and let-7d-3p could contribute to cardiac protection by targeting HMGA2 (21). Let-7f-5p was shown to ameliorate inflammation by targeting NLRP3 in bone marrow-derived mesenchymal stem cells in patients with systemic lupus erythematosus (22). Above all, most of the upregulated miRs are cell-damaging, and the majority of downregulated miRs are protective. We performed GO analysis to identify biological processes, cellular components, and molecular functions associated with the predicted target genes. We found that these miRNAs were greatly enriched in functions related to biological processes (aging and response to drug), cell components (cytoplasm and cytosol), and molecular functions (protein binding and protein kinase binding). KEGG analysis also highlighted the important pathways involved in the inflammation mechanism and cardiovascular disease, such as the HIF-1 signaling pathway, cGMP-PKG signaling pathway, and FoxO signaling pathway. HIF-1 plays an important role in coordinating gene expression with cardiac tissue oxygen tensions, and the decrease in oxygen availability is apparent during the course of ischemic heart disease (23). The role of HIF-1α in cardiac adaptation to ischemia has been analyzed (24), and increased protein levels of HIF-1α have been observed in heart samples from various models of pathological cardiac hypertrophy (25). Modulation of cGMP-PKG has entered clinical practice as a treatment for pulmonary hypertension or erectile dysfunction, and oxidation (ROS) attenuates PKG activation and protective signaling in cardiomyocytes (26). Patients with aortic stenosis and heart failure with reduced ejection fraction (HFrEF) showed reduced myocardial PKG activity and lower cGMP concentrations, which are associated with elevated myocardial nitrotyrosine levels and raised nitrosative/oxidative stress (27).

Some studies have reported that miR-29a is involved in heart diseases, such as cardiac hypertrophy (28), myocardial ischemia-reperfusion injury (29) and cardiac fibrosis (30). In a recent study, researchers found that mice deficient in miR-29a/b1 develop vascular remodeling, systemic hypertension and HF with preserved ejection fraction. The absence of miR-29 triggers the upregulation of PGC1α, which is overexpressed in hearts from patients with HF and contributes to cardiac disease (31). However, in our present study, the expression level of miR-29a showed no correlation with the change in NT-pro BNP, and the ROC analysis also indicated that it was not suitable as a biomarker. MiR-212-3p has been demonstrated to play

complicated roles in several pathological processes, such as neuropathic pain (32), ovarian cancer (33), and late-onset Alzheimer's disease (34). MiR-212/132 null mice are protected from pressure-overload-induced heart failure, whereas cardiomyocyte-specific overexpression of the miR-212/132 family leads to pathological cardiac hypertrophy, heart failure and death in mice. Both miR-212 and miR-132 directly target the anti-hypertrophic and pro-autophagic FoxO3 transcription factor and overexpression of these miRNAs leads to hyperactivation of pro-hypertrophic calcineurin/NFAT signaling and an impaired autophagic response upon starvation (35). Several studies have shown that miR-212-3p has a protective effect on the heart. Overexpression of miR-212 could inhibit the PI3K/Akt signaling pathway, thus decreasing cardiomyocyte apoptosis, promoting vascular regeneration and alleviating ventricular remodeling in rats with myocardial infarction (36). The chemotherapy drug doxorubicin can induce myofibril damage and cardiac atrophy, and overexpression of the miR-212/132 family reduces the development of doxorubicin-induced cardiotoxicity, indicating that it is a therapeutic method to limit doxorubicin-mediated adverse cardiac effects (37). In an earlier study, deletion of the miR-212/132 cluster increased endothelial vasodilatory function and improved angiogenic responses during postnatal development and in adult mice (35). However, until now, no study has reported the relationship between MiR-212 and right heart failure. Our results revealed that plasma MiR-212-3p levels correlated well with NT-pro BNP, which could assess heart function. PAH rats with acute inflammation showed lower levels of MiR-212-3p in plasma than PAH rats, and similar results were obtained from PAH patients. Importantly, the level of plasma miR-212-3p was significantly decreased along with the elevation of NT-pro BNP. These results indicated that plasma miR-212-3p might be a potential biomarker for heart failure and a useful marker in PAH patients with reduced heart function.

The present study has several limitations. The number of patient samples was small, and large scale studies will be needed in the future. Further experimental studies are needed to explore the mechanisms of the downregulation of MiR-212-3p. It is also a limitation that only plasma miRNA could be reproducibly validated in human PAH plasma samples. We should use other PAH models such as chronic hypoxia model to screen more PAH biomarkers to make up for too few markers screened by a single model.

The samples of PAH patients from other ethnic population samples should be investigated also. The problem of low miRNA reproducibility between patients and animal models may be due to multiple reasons. Gene expression is affected by many factors and it is difficult to achieve complete reproducibility. Maybe miRNAs in PAH plasma samples should be sequenced.

In conclusion, our study identified differentially expressed miRNAs between PAH rats and LPS-treated PAH rats by microarray analysis. The miR-212a-3p level was found to be decreased in the plasma of PAH patients after surgery compared to that before surgery. Furthermore, the plasma miR-212a-3p level in PAH patients was negatively correlated with NT-pro BNP levels. Since miRNA has high stability in plasma, miR-212a-3p can be accessed easily. miR-212a-3p may be considered a novel early diagnostic marker and treatment target that reflects the degree of the reduction in heart function in patients with PAH.

Acknowledgments

Footnote

Reporting Checklist: The authors have completed the ARRIVE reporting checklist. Available at http://dx.doi.org/10.21037/atm-20-1653a

Data Sharing Statement: Available at http://dx.doi.org/10.21037/atm-20-1653a

Conflicts of Interest: All authors have completed the ICMJE uniform disclosure form (available at http://dx.doi.org/10.21037/atm-20-1653a). The authors have no conflicts of interest to declare.

Ethical Statement: The authors are accountable for all aspects of the work in ensuring that questions related to the accuracy or integrity of any part of the work are appropriately investigated and resolved. The study was conducted in accordance with the Declaration of Helsinki (as revised in 2013). The study was approved by the

Institutional Review Board and Ethics Committee of Xiangya Hospital Central South University (201303311), and informed consent was obtained from patients. Experiments were performed under a project license (permit number: 201711997) granted by Ethics Committee for Animal Research of Xiangya Hospital of Central South University, in compliance with the recommendations of national and international animal care and ethical guidelines for the care and use of animals.

Open Access Statement: This is an Open Access article distributed in accordance with the Creative Commons Attribution-NonCommercial-NoDerivs 4.0 International License (CC BY-NC-ND 4.0), which permits the non-commercial replication and distribution of the article with the strict proviso that no changes or edits are made and the original work is properly cited (including links to both the formal publication through the relevant DOI and the license). See: https://creativecommons.org/licenses/by-nc-nd/4.0/.

References

1. Sztrymf B, Souza R, Bertoletti L, et al. Prognostic factors of acute heart failure in patients with pulmonary arterial hypertension. Eur Respir J 2010;35:1286-93.
2. Zhang J, Cao Y, Gao X, et al. Lipopolysaccharide acutely suppresses right-ventricular strain in rats with pulmonary artery hypertension. Pulm Circ 2018;8:2045893217744504.
3. Ambros V. The functions of animal microRNAs. Nature 2004;431:350-5.
4. Trotta MC, Ferraro B, Messina A, et al. Telmisartan cardioprotects from the ischaemic/hypoxic damage through a miR-1-dependent pathway. J Cell Mol Med 2019;23:6635-45.
5. Schulte C, Barwari T, Joshi A, et al. Comparative Analysis of Circulating Noncoding RNAs Versus Protein Biomarkers in the Detection of Myocardial Injury. Circ Res 2019;125:328-40.
6. Dal-Pra S, Hodgkinson CP, Mirotsou M, et al. Demethylation of H3K27 Is Essential for the Induction of Direct Cardiac Reprogramming by miR Combo. Circ Res 2017;120:1403-13.
7. He X, Ji J, Wang T, et al. Upregulation of Circulating miR-195-3p in Heart Failure. Cardiology 2017;138:107-14.
8. Li G, Song Y, Li YD, et al. Circulating miRNA-302 family members as potential biomarkers for the diagnosis of acute heart failure. Biomark Med 2018;12:871-80.
9. Lin X, Zhang S, Huo Z. Serum Circulating miR-150 is a Predictor of Post-Acute Myocardial Infarction Heart Failure. Int Heart J 2019;60:280-6.
10. Cao Y, Yang Y, Wang L, et al. Analyses of long non-coding RNA and mRNA profiles in right ventricle myocardium of acute right heart failure in pulmonary arterial hypertension rats. Biomed Pharmacother 2018;106:1108-15.
11. Marra AM, Benjamin N, Cittadini A, et al. When Pulmonary Hypertension Complicates Heart Failure. Heart Fail Clin 2020;16:53-60.
12. Ryan JJ, Archer SL. Emerging concepts in the molecular basis of pulmonary arterial hypertension: part I: metabolic plasticity and mitochondrial dynamics in the pulmonary circulation and right ventricle in pulmonary arterial hypertension. Circulation 2015;131:1691-702.
13. Roger VL, Go AS, Lloyd-Jones DM, et al. Executive summary: heart disease and stroke statistics--2012 update: a report from the American Heart Association. Circulation 2012;125:188-97.
14. Badagliacca R, Ghio S, Correale M, et al. Prognostic significance of the echocardiographic estimate of pulmonary hypertension and of right ventricular dysfunction in acute decompensated heart failure. A pilot study in HFrEF patients. Int J Cardiol 2018;271:301-5.
15. Wu J, Qin XH, Hou ZX, et al. [miR-494-3p reduces insulin sensitivity in diabetic cardiomyocytes by down-regulation of insulin receptor substrate 1]. Sheng Li Xue Bao 2019;71:271-8.
16. Costantino S, Akhmedov A, Melina G, et al. Obesity-induced activation of JunD promotes myocardial lipid accumulation and metabolic cardiomyopathy. Eur Heart J 2019;40:997-1008.
17. Qin Y, Guo X, Yu Y, et al. Screening key genes and miRNAs in sepsis by RNA-sequencing. J Chin Med Assoc 2020;83:41-7.
18. Zhang J, Li SF, Chen H, et al. Role of miR-106b-5p in the regulation of gene profiles in endothelial cells. Beijing Da Xue Xue Bao Yi Xue Ban 2019;51:221-7.
19. Li Z, Yuan B, Pei Z, et al. Circ_0136474 and MMP-13 suppressed cell proliferation by competitive binding to miR-127-5p in osteoarthritis. J Cell Mol Med 2019;23:6554-64.
20. Raheja R, Regev K, Healy BC, et al. Correlating serum micrornas and clinical parameters in amyotrophic lateral sclerosis. Muscle Nerve 2018;58:261-9.
21. Wong LL, Saw EL, Lim JY, et al. MicroRNA Let-7d-3p Contributes to Cardiac Protection via Targeting HMGA2. Int J Mol Sci 2019;20:1522.

22. Tan W, Gu Z, Leng J, et al. Let-7f-5p ameliorates inflammation by targeting NLRP3 in bone marrow-derived mesenchymal stem cells in patients with systemic lupus erythematosus. Biomed Pharmacother 2019;118:109313.

23. Semenza GL. O2-regulated gene expression: transcriptional control of cardiorespiratory physiology by HIF-1. J Appl Physiol (1985) 2004;96:1173-7; discussion 1170-2.

24. Eckle T, Kohler D, Lehmann R, et al. Hypoxia-inducible factor-1 is central to cardioprotection: a new paradigm for ischemic preconditioning. Circulation 2008;118:166-75.

25. Krishnan J, Suter M, Windak R, et al. Activation of a HIF1alpha-PPARgamma axis underlies the integration of glycolytic and lipid anabolic pathways in pathologic cardiac hypertrophy. Cell Metab 2009;9:512-24.

26. Nakamura T, Ranek MJ, Lee DI, et al. Prevention of PKG1alpha oxidation augments cardioprotection in the stressed heart. J Clin Invest 2015;125:2468-72.

27. van Heerebeek L, Hamdani N, Falcao-Pires I, et al. Low myocardial protein kinase G activity in heart failure with preserved ejection fraction. Circulation 2012;126:830-9.

28. Zhang S, Yin Z, Dai FF, et al. miR-29a attenuates cardiac hypertrophy through inhibition of PPARdelta expression. J Cell Physiol 2019;234:13252-62.

29. Ding S, Liu D, Wang L, et al. Inhibiting microRNA-29a protects myocardial ischemia-reperfusion injury by targeting SIRT1 and regulating NLRP3 and apoptosis pathway. J Pharmacol Exp Ther 2020;372:128-35.

30. Qin RH, Tao H, Ni SH, et al. microRNA-29a inhibits cardiac fibrosis in Sprague-Dawley rats by downregulating the expression of DNMT3A. Anatol J Cardiol 2018;20:198-205.

31. Caravia XM, Fanjul V, Oliver E, et al. The microRNA-29/PGC1alpha regulatory axis is critical for metabolic control of cardiac function. PLoS Biol 2018;16:e2006247.

32. Li Y, Zhang X, Fu Z, et al. microRNA-212-3p attenuates neuropathic pain via targeting sodium voltage-gated channel alpha subunit 3 (NaV 1.3). Curr Neurovasc Res 2019;16:465-72.

33. Lu X, Wang F, Fu M, et al. Long non-coding RNA KCNQ1OT1 accelerates the progression of ovarian cancer via microRNA-212-3/ LCN2 axis. Oncol Res 2020;28:135-46.

34. Herrera-Espejo S, Santos-Zorrozua B, Alvarez-Gonzalez P, et al. A Systematic Review of MicroRNA Expression as Biomarker of Late-Onset Alzheimer's Disease. Mol Neurobiol 2019;56:8376-91.

35. Kumarswamy R, Volkmann I, Beermann J, et al. Vascular importance of the miR-212/132 cluster. Eur Heart J 2014;35:3224-31.

36. Ren N, Wang M. microRNA-212-induced protection of the heart against myocardial infarction occurs via the interplay between AQP9 and PI3K/Akt signaling pathway. Exp Cell Res 2018;370:531-41.

37. Gupta SK, Garg A, Avramopoulos P, et al. miR-212/132 Cluster Modulation Prevents Doxorubicin-Mediated Atrophy and Cardiotoxicity. Mol Ther 2019;27:17-28.

Table S1 Echocardiographic ventricular function variables in rats.

Variables	PAH	PAH+LPS	P value
TAPSE (mm)	2.26±0.17	1.53±0.25	0.026
RVEDD (mm)	5.337±0.019	6.097±0.298	0.023
sPAP (mmHg)	80. 0±1.6	98.7±1.7	<0.001
Strain %			
Basal RV free wall	−11.10±0.51	−6.57±2.04	0.038
Mid RV free wall	−15.67±4.62	−5.30±2.51	0.049
Basal septal wall	−17.93±2.74	−10.00±1.77	0.026
Mid septal wall	−15.63±1.96	−13.73±5.50	0.669
Strain rate I/S			
Basal RV free wall	−5.36±0.58	−3.50±0.51	0.027
Mid RV free wall	−4.83±0.62	−2.93±0.31	0.018
Basal septal wall	−5.89±1.91	−3.46±0.25	0.149
Mid septal wall	−3.90±0.97	−3.90±0.76	0.521
BNP (pg/mL)	200.77±22.82	844.14±29.88	<0.001

Values are the mean ± SD. n=3. PAH: PAH rats; PAH+LPS: PAH rats with LPS treatment. TAPSE, tricuspid annular plane systolic excursion; RVEDD, right ventricle end diastolic diameter; sPAP, pulmonary artery systolic pressure.

Table S2 The readouts of MiR-212-3p quantification and NT-pro BNP of PAH patients

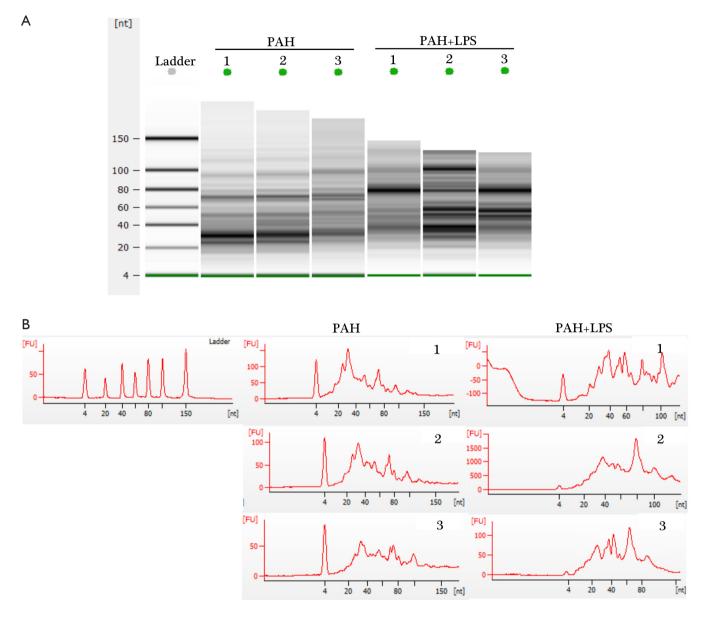| Patient	MiR-212-3P (ΔCt)		NT-proBNP (pg/mL)	
	Before surgery	After surgery	Before surgery	After surgery
A	8.50	6.20	443	801
B	10.38	8.02	9,245	2,356
C	10.65	6.22	365	509
D	10.12	9.17	750	4,519
E	9.37	8.04	1,443	4,561
F	9.60	6.76	504	1,503
G	11.39	10.53	3,085	2,803
H	9.93	11.79	2,357	7,250
I	9.25	12.41	5,141	5,207
J	9.02	5.35	2,681	7,263
K	11.31	5.75	1,739	5,002
L	11.93	7.81	379	1,404
M	9.36	8.49	2,107	1,888
N	9.36	10.30	453	693
O	12.09	9.64	5,499	2,764

Ct, cycle threshold.

Figure S1 RNA Quality Control. (A) A total RNA sample was degraded for varying times and the resulting samples were analyzed on the Agilent 2100 bioanalyzer. (B) RNA Integrity Number (RIN) visualization.
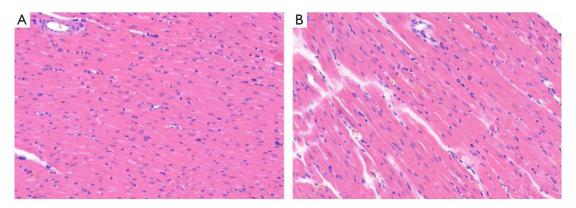
Figure S2 Representative of HE staining myocardium of right ventricle from a control rat (A) and PAH rat (B). Scale bar =50 µm.

http://dx.doi.org/10.21037/atm-20-1653A